AFML-TR-76-176

AN INTERPOLATIVE MODEL FOR ELEVATED TEMPERATURE FATIGUE CRACK PROPAGATION

PRATT & WHITNEY AIRCRAFT GROUP
WEST PALM BEACH, FLORIDA 33402

NOVEMBER 1976

FINAL TECHNICAL REPORT AFML-TR-76-176
FINAL REPORT FOR PERIOD 3 FEBRUARY 1975 through 31 JULY 1976

Approved for public release; distribution unlimited

AIR FORCE MATERIALS LABORATORY
AIR FORCE SYSTEMS COMMAND
WRIGHT-PATTERSON AIR FORCE BASE, OHIO 45433

NOTICE

When government drawings, specifications, or other data are used for any purpose other than in connection with a definitely related government procurement operation, the United States Government thereby incurs no responsibility nor any obligation whatsoever; and the fact that the government may have formulated, furnished, or in any way supplied the said drawings, specifications, or other data, is not to be regarded by implication or otherwise as in any manner licensing the holder or any other person or corporation, or conveying any rights or permission to manufacture, use, or sell any patented invention that may in any way be related thereto.

This report has been reviewed by the Information Office (IO) and is releasable to the National Technical Information Service (NTIS). At NTIS, it will be available to the general public, including foreign nationals.

This technical report has been reviewed and is approved for publication.

WALTER H. REIMANN
Project Engineer

FOR THE COMMAND

GAIL E. EICHELMAN
Metals Behavior Branch
Metals & Ceramics Division

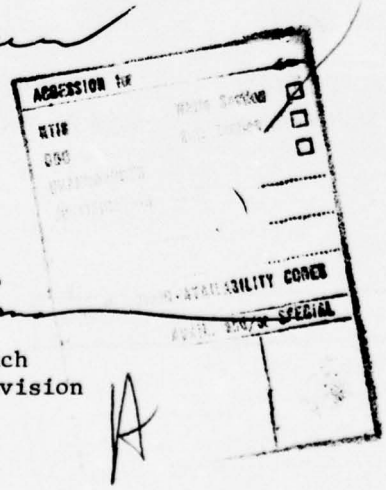

Copies of this report should not be returned unless return is required by security consideration, contractual obligations, or notice on a specific document.

UNCLASSIFIED

SECURITY CLASSIFICATION OF THIS PAGE (When Data Entered)

REPORT DOCUMENTATION PAGE		READ INSTRUCTIONS BEFORE COMPLETING FORM
1. REPORT NUMBER AFML-TR-76-176	2. GOVT ACCESSION NO.	3. RECIPIENT'S CATALOG NUMBER
4. TITLE (and Subtitle) An Interpolative Model for Elevated Temperature Fatigue Crack Propagation		5. TYPE OF REPORT & PERIOD COVERED Final for Phase I 3 Feb 75 - 31 Jul 76 6. PERFORMING ORG. REPORT NUMBER FR-8042
7. AUTHOR(s) C.G. Annis, Jr., R.M. Wallace, and D.L. Sims		8. CONTRACT OR GRANT NUMBER(s) F33615-75-C-5097
9. PERFORMING ORGANIZATION NAME AND ADDRESS Pratt & Whitney Aircraft Group Government Products Division West Palm Beach, Florida 33402		10. PROGRAM ELEMENT, PROJECT, TASK AREA & WORK UNIT NUMBERS
11. CONTROLLING OFFICE NAME AND ADDRESS Air Force Materials Laboratory Air Force Systems Command Wright-Patterson AFB, Ohio 45433		12. REPORT DATE November 1976 13. NUMBER OF PAGES 35
14. MONITORING AGENCY NAME & ADDRESS (if different from Controlling Office) Air Force Materials Laboratory Air Force Systems Command Wright-Patterson AFB, Ohio 45433		15. SECURITY CLASS. (of this report) Unclassified 15a. DECLASSIFICATION/DOWNGRADING SCHEDULE

16. DISTRIBUTION STATEMENT (of this Report)

Approved for public release, distribution unlimited.

17. DISTRIBUTION STATEMENT (of the abstract entered in Block 20, if different from Report)

18. SUPPLEMENTARY NOTES

19. KEY WORDS (Continue on reverse side if necessary and identify by block number)

Fracture Mechanics,
IN-100,
Interpolative Model,
Crack Propagation,
Hyperbolic Sine

20. ABSTRACT (Continue on reverse side if necessary and identify by block number)

A flexible alternative to the familiar Paris equation has been developed for the interpolative analysis of elevated temperature fatigue crack propagation data. The model is based on the hyperbolic sine equation,

$$\log (da/dn) = C_1 \sinh (C_2 (\log (\Delta K) + C_3)) + C_4,$$

and the coefficients are shown to be simple functions of test frequency, stress

over

DD FORM 1 JAN 73 1473 EDITION OF 1 NOV 65 IS OBSOLETE

UNCLASSIFIED

SECURITY CLASSIFICATION OF THIS PAGE (When Data Entered)

ratio, and temperature. This methodology has been successfully used to describe crack propagation characteristics of selected nickel-base, titanium, and steel alloys.

FOREWORD

The major portion of this work was performed under Air Force Materials Laboratory Contract F33615-75-C-5097, "Application of Advanced Fracture Mechanics at Elevated Temperatures." Dr. W. H. Reimann is the project engineer. The program is being conducted in the Materials Laboratories, Pratt & Whitney Aircraft Government Products Division, West Palm Beach, Florida. Mr. M. C. VanWanderham, General Supervisor Applied Mechanics, is program manager and Mr. R. M. Wallace, Group Leader Component Life Analysis, is the principal investigator.

SUMMARY

An interpolative model has been developed for the analysis of elevated temperature fatigue crack propagation data. The model presented here has been successfully used to describe the parametric effects of three fundamental influences on crack propagation: frequency (ν), stress ratio (R), and temperature (T).

This interpolative model is based on the hyperbolic sine equation,

$$\log (da/dn) = C_1 \sinh (C_2 (\log (\Delta K) + C_3)) + C_4$$

where the coefficients are simple empirical functions of test frequency, stress ratio, and temperature:

C_1 = material constant
$C_2 = f_2 (R, \nu, T)$
$C_3 = f_3 (C_4, \nu, R)$
$C_4 = f_4 (\nu, R, T)$

Although this model has been successfully used to describe the characteristics of selected nickel-base, titanium, and steel alloys, the material characterized is IN-100 forged using the GATORIZING™ process. IN-100 is an advanced turbine disk alloy used in the F100 turbofan engine.

CONTENTS

ILLUSTRATIONS

ILLUSTRATIONS (Continued)

SECTION I

INTRODUCTION

Historically, the methods for predicting low-cycle fatigue (LCF) life have produced conservative underestimations of total useful life, resulting in costly early replacement of LCF limited gas turbine engine rotating components. Accurate total LCF life predictions must consider (1) the initiation of an actively propagating macrocrack, (2) fatigue crack propagation under constant maximum load, and (3) deviations in propagation behavior (acceleraiton and/or retardation) caused by major load excursions.

Exclusive of retardation effects, which are not considered here, there are three fundamental parametric influences on crack propagation: frequency (ν), stress ratio (R), and temperature (T).

Engine hardware operates under complicated stress-time-temperature spectra, but laboratory testing must be done at selected conditions because of cost and time limitations. To describe crack propagation at conditions where test data does not exist, an interpolative crack propagation model is necessary.

A flexible alternative to the familiar Paris equation has been developed for the interpolative analysis of elevated temperature fatigue crack propagation data. The model is based on the hyperbolic sine equation,

$$\log (da/dn) = C_1 \sinh (C_2 (\log (\Delta K) + C_3)) + C_4, \qquad \text{eqn 1}$$

and the coefficients are shown to be simple functions of test frequency, stress ratio, and temperature.

The resulting model provides the vehicle for applying linear elastic fracture mechanics (LEFM) to LCF residual life predictions of disk components subjected to missions of varying cyclic frequency, stress ratio, and temperature. This assumes the limits of applicability of LEFM at elevated temperature have been defined.

All fracture mechanics evaluations were performed on GATORIZED™ IN-100, an advanced nickel-base turbine disk alloy used in the F100 turbofan engine. Specimens specifically designated to this contract were machined from heat BANQ-499, but a significant amount of crack propagation data existed for this alloy prior to the start of this program which is also used in the analyses. Heat treatment consists of solutionization at 2050°F, stabilization at 1600°F and 1800°F, and precipitation hardening at 1200°F and 1400°F. Typical chemical composition is 0.07C - 12.4Cr - 18.5Co - 3.2Mo - 4.32Ti - 4.98Al - 0.78V - 0.02B - 0.06Zr - balance nickel.

Tensile, stress rupture, and creep test results for two forgings from this heat (499-A2A and 499-A2B) are given in Table I.

The results of this program are currently being used at Pratt & Whitney Aircraft/Florida, in the design and analysis of current and future engine hardware.

TABLE I. MECHANICAL PROPERTIES OF TXWO IN-100 PANCAKE FORGINGS AFML CONTRACT F33615-75-C-5097

Disk No.	Temperature (°F)	Yield Strength (ksi)	Ultimate Tensile Strength (ksi)	EL (%)	RA (%)
499-A2A	RT	164.5	232.4	22.0	22.2
499-A2A	1300	157.2	177.0	14.0	22.3
499-A2B	RT	164.9	232.0	22.0	21.5
499-A2B	1300	156.0	179.1	14.7	16.4

Stress Rupture Properties

Disk No.	Temperature (°F)	Stress (ksi)	Life (hr)	EL (%)	RA (%)
499-A2A	1350	95	28.0	10.6	15.9
499-A2B	1350	95	18.1	8.1	15.6
499-A2B	1350	95	19.5	8.0	8.2
499-A2B	1350	95	19.3	6.7	12.9

Creep Rupture Properties

Disk No.	Temperature (°F)	Stress (ksi)	0.1% hr)	0.2% (hr)	Total Life (hr)
499-A2A	1300	80	-	175 5	233.2*
499-A2B	1300	80	114.5	142.5	143.2*

*Test Discontinued.

SECTION II

THE BASIC HYPERBOLIC SINE MODEL

A flexible alternative to the familiar Paris equation has been developed for the analysis of fatigue crack propagation data. The model is based on the hyperbolic sine equation,

$$\log (da/dn) = C_1 \sinh (C_2 (\log (\Delta K) + C_3)) + C_4. \qquad \text{eqn 1}$$

The coefficients are empirical functions of test frequency, stress ratio, and temperature.

A. CHARACTERISTICS OF THE SINH

The hyperbolic sine is defined as

$$y = \sinh x = \frac{e^x - e^{-x}}{2} \qquad \text{eqn 2}$$

and when presented on cartesian coordinates it appears as shown in Figure 1. The function is zero at $x = 0$ and has its inflection there.

The introduction of the four regression coefficients, C_1 through C_4, permits relocation of the point of inflection and scaling of both axes. In the equation

$$(y - C_4) = \sinh (x + C_3), \qquad \text{eqn 3}$$

C_3 establishes the horizontal location of the hyperbolic sine point of inflection and C_4 locates its vertical position.

To scale the axes, C_1 and C_2 are introduced

$$\frac{(y - C_4)}{C_1} = \sinh (C_2 (x + C_3)) \qquad \text{eqn 4}$$

which can be rewritten as

$$y = C_1 \sinh (C_2 (x + C_3)) + C_4 \qquad \text{eqn 5}$$

of which equation 1 is a special case where $y = \log (da/dn)$ and $x = \log (\Delta K)$. Note that C_3 has units of $\log (\Delta K)$ and C_4 has units of $\log (da/dn)$; C_1 and C_2 are dimensionless and can be conceptualized as stretching the curve vertically and horizontally, respectively. Experience indicates that, for a given material, C_1 can be fixed without adversely affecting model flexibility. For IN-100, C_1 has a fixed value of 0.5.

B. QUALITATIVE EFFECT OF TEST FREQUENCY, STRESS RATIO, AND TEMPERATURE

Experience with turbine disk alloys indicates that increasing test frequency, while holding stress ratio and temperature constant, produces crack growth curves similar in shape but shifted along a nearly vertical line passing through the points of inflection. Section III will demonstrate that the location of these inflection points is linearly related to test frequency.

Changes in stress ratio produce crack growth curves which are also shifted along a line passing through the points of inflection but with a shallower (but not horizontal) slope as compared to test frequency. Another simple linear expression will be presented, relating these points of inflection to stress ratio.

Figure 2 schematically depicts the qualitative effects of frequency and stress ratio on the hyperbolic sine representation of crack growth rate.

Investigation of the oxidation kinetics of IN-100 at elevated temperatures shows that crack propagation under representative cyclic conditions is more dependent on oxidation than creep phenomena. As with the frequency and stress ratio models, a simple linear equation relates temperature with the hyperbolic sine representation of crack propagation. Section III investigates the quantitative effects of temperature, and addresses the corroboration of empirical observation through kinetics studies.

C. PHYSICAL SIGNIFICANCE OF THE SINUSOIDAL SHAPE OF IN-100 CRACK GROWTH CURVES

A thin-foil electron microscopy study was performed on an IN-100 specimen to gain physical insight into the sinusoidal shape of the crack growth curves. Thin-foils were prepared from areas adjacent to the fracture surface of a specimen tested at 1200°F, R = 0.1, 10 cps. The primary dislocation sources changed from the gamma phase, to MC carbides, to grain boundaries with increasing applied stress intensity, ΔK. Figures 3, 4, and 5 present electron micrographs that depict these mechanistic changes. The approximate inflection point at this cyclic frequency, $\Delta K = 27$ ksi$\sqrt{\text{inch}}$, coincides with the point grain boundary dislocation sources are activated.

This mechanism probably accelerates the grain boundary oxidation kinetics, thereby creating an acceleration in crack growth rate, thus changing the curve from concave to convex.

Figure 6 presents crack propagation data for IN-100 at room temperature, R = 0.1. These were obtained from a 0.5 inch thick modified compact tension specimen. Comparing these data with Group 2 in Figure 7, it can be noted that an inflection point is nonexistent at room temperature as compared to an equivalent range of data at elevated temperatures. At room temperature, where the primary fracture mode is transgranular with virtually no environmental interaction, an inflection point would only be expected when tensile overstress begins to dominate fatigue on each cycle. The difference in curve shapes at room and elevated temperatures has also been noted in austenitic stainless steels (Reference 1). The interactive effects of dislocation mechanisms and environment requires further investigation.

SECTION III

QUANTITATIVE EFFECTS OF CYCLIC FREQUENCY, STRESS RATIO, AND TEMPERATURE ON CRACK GROWTH IN IN-100

There are three fundamental parametric influences on fatigue crack propagation: test frequency, stress ratio and temperature. The quantitative effects of these are mathematically described using the hyperbolic sine model. The analysis presented here considers only propagation under constant peak loading.

All fracture mechanics evaluations were performed on GATORIZED IN-100, an advanced turbine disk alloy used in the F100 turbofan engine. IN-100 is a nickel-base powder metallurgy alloy, and when superplastically forged with the GATORIZING™ process becomes a fine grained (ASTM 12-14), isotropic material.

A. FREQUENCY EFFECTS ON FATIGUE CRACK GROWTH

The qualitative effect of test frequency on crack propagation rate is to shift a growth rate curve along a nearly vertical line passing through the inflection. For IN-100, this correlation line has an approximate slope of 18, at 1200°F, R = 0.1 (Figure 7). It is interesting to note that this is also the slope of the Paris equation describing the early (threshold region) data taken at three test frequencies, 20 Hz, 10 cpm, and 2-minute dwell, at this temperature and stress ratio. The tangent to the hyperbolic sine representing the high-frequency data also has this approximate slope when evaluated at threshold.

This behavior of crack growth curves at different frequencies is not peculiar to IN-100. The frequency effects on type 304 stainless steel at 1000°F, described by James (Reference 2), could be interpreted as a shift along a correlation line having the same slope displayed by early data at each frequency.

Figure 8 illustrates the simple linear relationship between C_3 and C_4 with changing frequency. To use the hyperbolic sine to describe crack growth at differing frequencies, it is necessary to relate the coefficients to frequency. Plotting C_4 as a logarithmic function of cycle duration, $1/\nu$, provides the desired relationship (Figure 9). Relating C_2 to log $(1/\nu)$ (Figure 9) completes model development.

Another conclusion from the study of this multifrequency data is that increasing frequency lowers the crack propagation threshold. Laboratory observation shows that existing cracks do not propagate in a predictable manner at frequencies and stress intensities defining the Paris threshold line, Figure 7.

B. STRESS RATIO EFFECTS ON CRACK PROPAGATION

The qualitative effect of stress ratio is to shift a growth rate curve along a line passing through the inflection points. The experimental observation that this shift is not horizontal (Figures 10 and 11) forms the basis for stress ratio modeling with the hyperbolic sine.

Figure 10 presents 10 cpm, 1200°F data, generated at three stress ratios: R = 0.1, R = 0.5, and R = 0.8. The points of inflection lie along a line sloping downward to the left as stress ratio is increased. Similarly, Figure 11 presents the 20 Hz, 1200°F data, generated at the same three stress ratios. The trend of data shift with changing stress ratio is obscured by the steeper slope of

the correlation line. To circumvent this difficulty, the crack growth rate data are plotted as a function of maximum stress intensity, K_{max}, rather than applied stress intensity, ΔK. Figures 12 and 13 present the 10 cpm and 20 Hz data, respectively, as functions of K_{max}. The linear relationships between C_3 and C_4 are obvious.

To investigate the relationship between these coefficients and stress ratio, C_3 plotted against log (1-R) is presented in Figure 14. Both frequencies exhibit linear variation of C_3 with log (1-R).

This analysis provides a simple method of generating a crack growth curve for any positive stress ratio. Coupled with the analysis presented in the preceding section, complete representation of crack propagation behavior at 1200°F is possible.

Considered next is the expansion of this model to encompass the effects of temperature.

C. EFFECT OF TEMPERATURE

At elevated temperatures, the driving force for crack growth is a function of input mechanical and thermal energy. Crack tip response depends on the relative roles played by mechanical fatigue, creep, and environment under representative operating conditions. To determine which mechanism dominates in the elevated temperature regime, activation energy analyses were performed where crack propagation data for IN-100 are plotted in Arrhenius diagrams. These analyses yielded useful information for modeling temperature effects with the hyperbolic sine model, but the crack growth rate vs inverse temperature display consistent deviation from linear behavior; therefore, the temperature model uses temperature, rather than its inverse, as the coefficient correlative parameter. The analysis is as follows.

The Arrhenius equation has the form:

$$da/dn = A \exp(-Q/R' T_{abs}) \qquad \text{eqn 6}$$

where A = function which includes a mechanical driving force
Q = apparent activation energy for the process
R' = universal gas constant
T_{abs} = absolute temperature

A recent internal P&WA/Florida study experimentally determined the oxidation rates for IN-100 in air at various elevated temperatures. The activation energy for parabolic oxidation is approximately 40 Kcal/ mole; linear oxidation kinetics are activated as low as 20 Kcal/mole. This study also revealed a change in oxidation kinetics near 1350°F, with an increase in oxidation activation energy above that temperature. For this reason, the temperature model for fatigue crack propagation is restricted to the range from 1000°F to 1350°F.

Linear kinetics are thought to control local fracture processes. By comparing the apparent activation energies for crack growth in IN-100 with those for oxidation and creep, a qualitative assessment can be made as to the relative contributions of mechanical, creep, and oxidation damage to the fatigue process.

Figures 15 and 16 illustrate the effects of temperature on crack propagation in IN-100, at two representative test frequencies, 10 cpm, and 2-minute dwell. To prepare Arrhenius diagrams, these figures are analyzed at 10 ksi$\sqrt{\text{inch}}$ increments of stress intensity and the corresponding crack growth rate is plotted versus inverse absolute temperature. Figures 17 and 18 present the resulting Arrhenius relationships, at 10 cpm and 2-minute dwell, respectively.

The slope of an Arrhenius line is equal to $-Q/R'$, where R' is the universal gas constant and Q is the apparent activation energy of the process rate being investigated. Note that the activation energies for crack propagation at a given frequency and stress ratio increase with increasing applied stress intensity, over the temperature range 1000°F to 1350°F (Figures 17 and 18).

Figures 17 and 18 display a consistent, subtle deviation from truly linear behavior: the 1200°F data are always below the linear regression representing 1000°F, 1200°F, and 1350°F. Because the variation is not random, it must have some physical cause. Referring to Figure 18, the dramatic increase in slope at 1350°F is a better representation of the activation energy at this temperature than the shallower slopes exhibited between 1000°F and 1350°F. Assuming linear behavior between 1000°F and 1200°F, and between 1400°F and 1350°F, consider a linear extrapolation from 1000°F through 1200°F to 1350°F. Consider also an extrapolation from 1400°F through 1350°F to intersection with the first extrapolation. This intersection occurs near 1340°F, regardless of stress intensity, an implication that the observed change in oxidation kinetics reported near 1350°F may actually occur at a slightly lower temperature. Further chemical investigations are currently in progress to augment the study of temperature effects.

Figure 19 compares the activation energies of fatigue crack propagation with those of secondary creep, linear oxidation and parabolic oxidation. Oxidation appears to dominate creep. Further testing in vacuum has substantiated this analysis. These results are consistent with those presented in Reference 4.

D. THE TEMPERATURE MODEL

A vertical line connects the points of inflection of the temperature model from 1000°F to 1400°F, stress ratio and frequency being constant. Figures 15 and 16 present the temperature data, da/dn vs ΔK, for 10 cpm and 2-minute dwell.

To correlate the sinh coefficients with temperature, C_2 and C_4 are plotted as functions of temperature, from 1000°F to 1350°F as shown in Figures 20 and 21. The C_1 remains fixed at 0.5, and C_3 does not change with temperature because the correlation line is vertical.

E. USING THE HYPERBOLIC SINE MODEL: INTERPOLATIVE CAPABILITY

The simple relationships presented describe the crack propagation behavior of IN-100, in air, at any stress ratio and frequency for temperatures between 1000°F and 1350°F. The computational procedure is schematically represented in Figure 22: First locate the coefficients on the 1200°F, R = 0.1 frequency model, position 1. Second, account for stress ratio effects by moving along a stress ratio model to position 2. Finally, C_2 and C_4 for the desired temperature are determined using $\partial C/\partial T$ from the temperature model, position 3.

A computer program is under development which will provide, as output, the four hyperbolic sine coefficients describing crack propagation behavior under the influence of input parameters; frequency, stress ratio, and temperature.

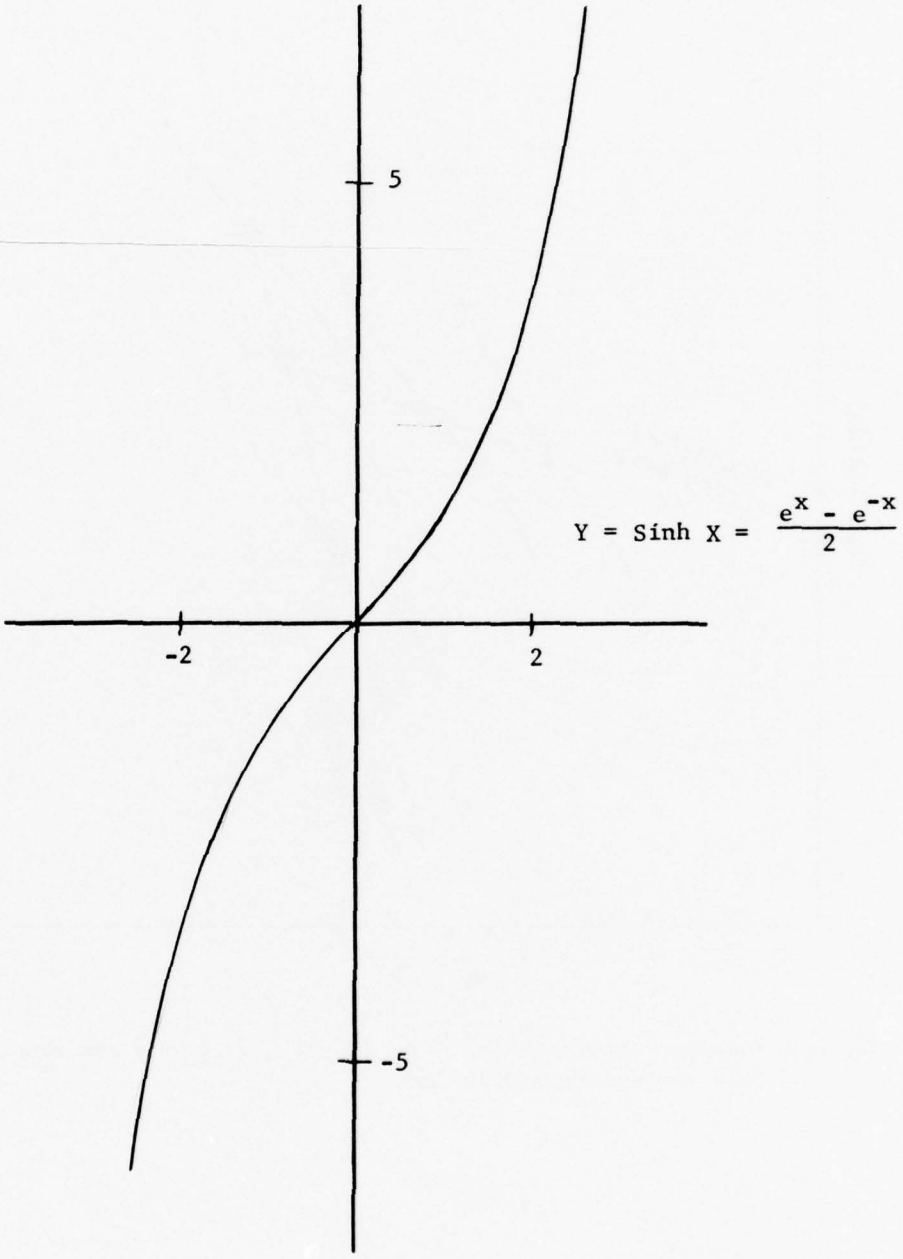

Figure 1. The Sinh on Cartesian Coordinates

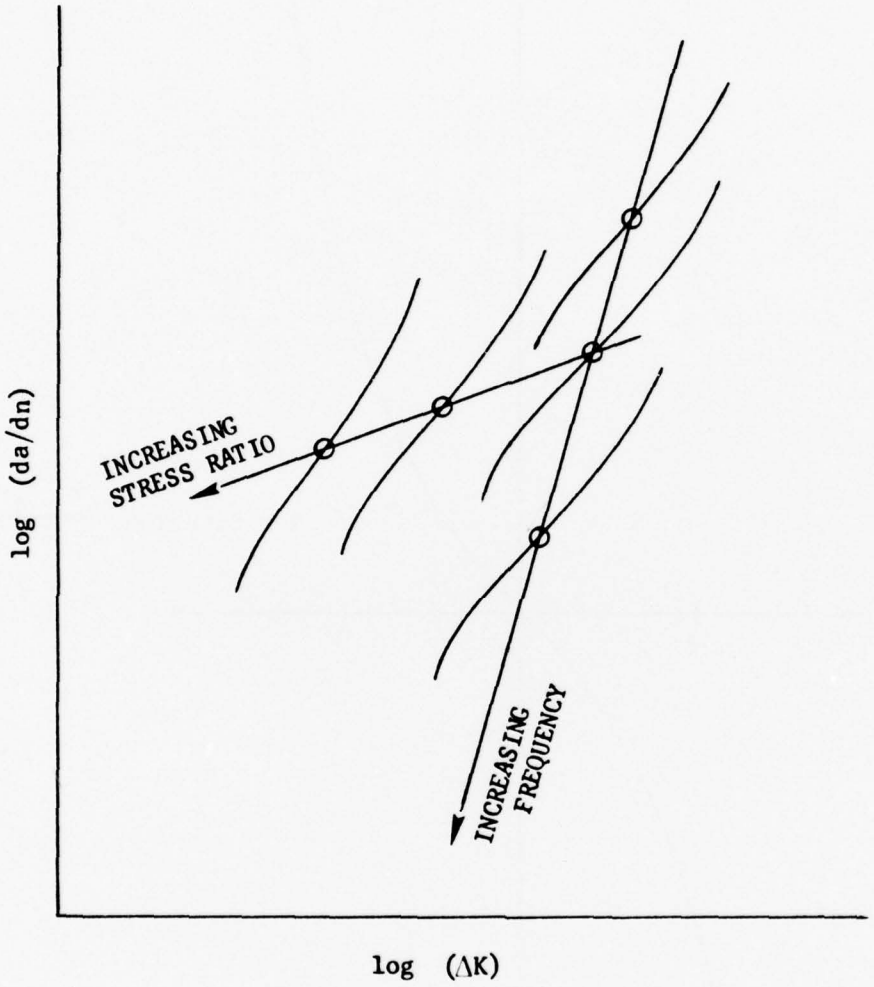

Figure 2. Schematic Representation of the Effects of Frequency and Stress Ratio on Crack Propagation Rate

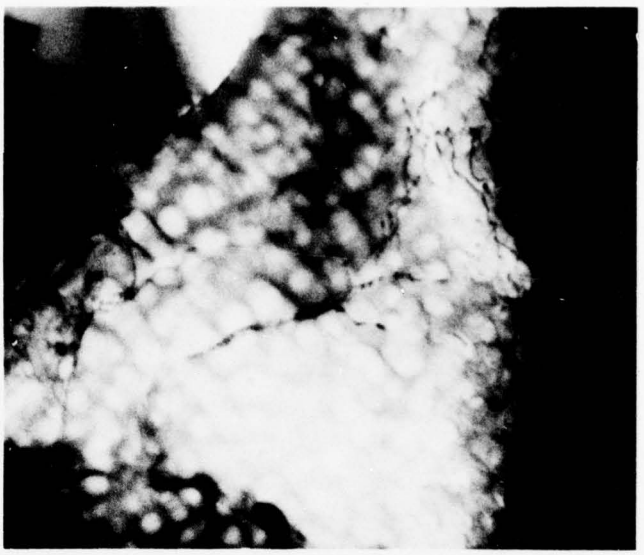

MAG 20,000×

Figure 3. Thin-Foil Electron Micrograph of IN-100 Specimen Tested at 1200°F, R = 0.1, 10 cpm. K_{max} = 18.0 ksi $\sqrt{inch}$. Note Dislocations Favor the Gamma Phase

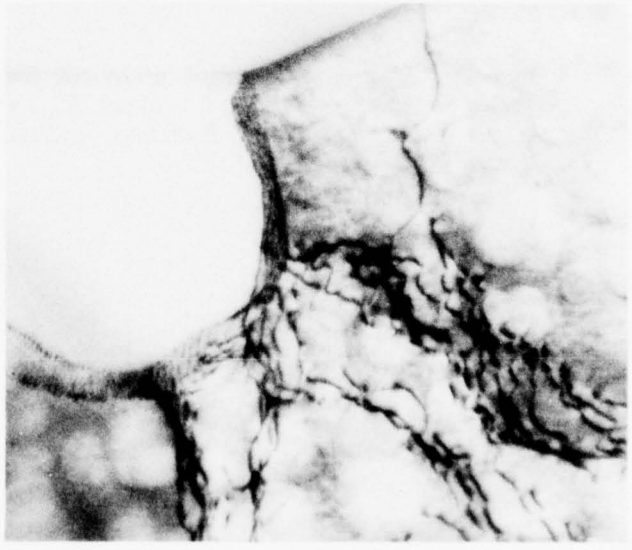

MAG 70,000×

Figure 4. Thin-Foil Electron Micrograph of IN-100 Specimen Tested at 1200°F, R = 0.1, 10 cpm. K_{max} = 29.5 ksi $\sqrt{inch}$. Note that MC carbides and Grain Boundaries are Dislocation Sources

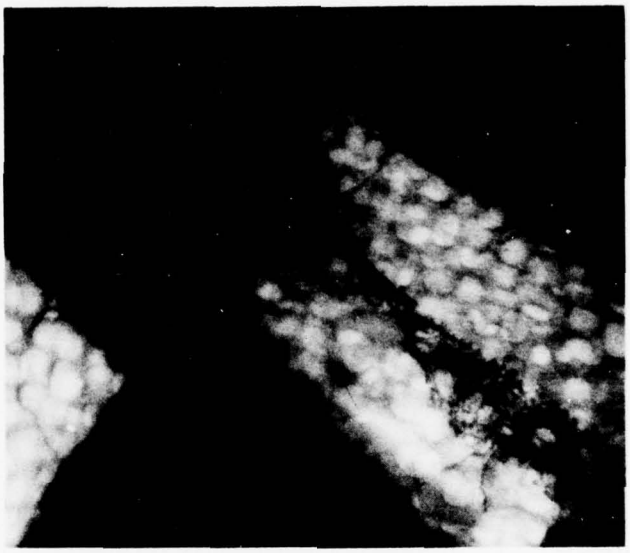

MAG 20,000×

Figure 5. Thin-Foil Electron Micrograph of IN-100 Specimen Tested at 1200°F, R = 0.1, 10 cps. K_{max} = 42 ksi $\sqrt{inch}$. Note that Grain Boundary is Dislocation Source

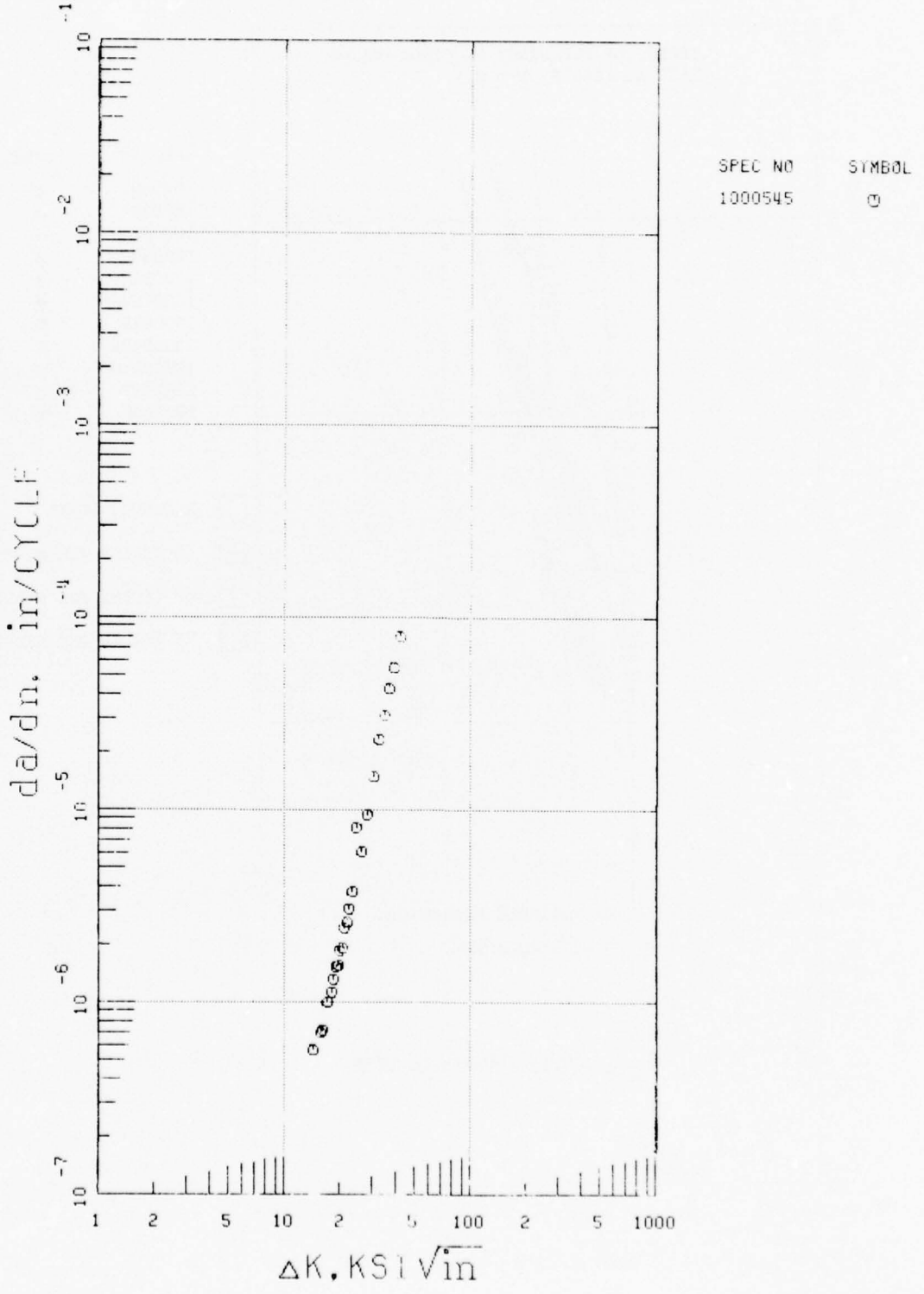

Figure 6. Crack Propagation Data for IN-100 at Room Temperature, R = 0.1

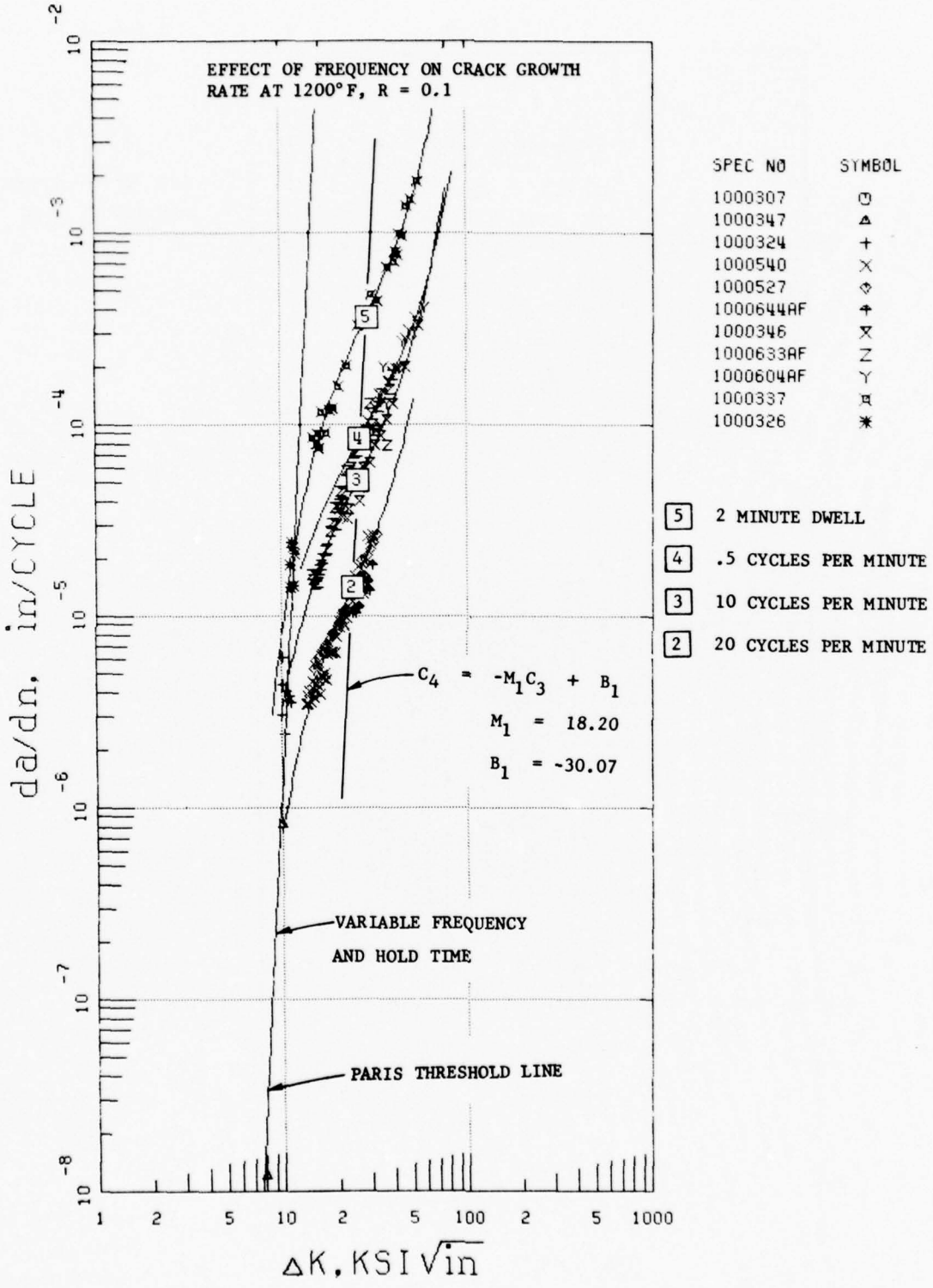

Figure 7. The Effect of Frequency on Crack Growth Rate at 1200°F, R = 0.1

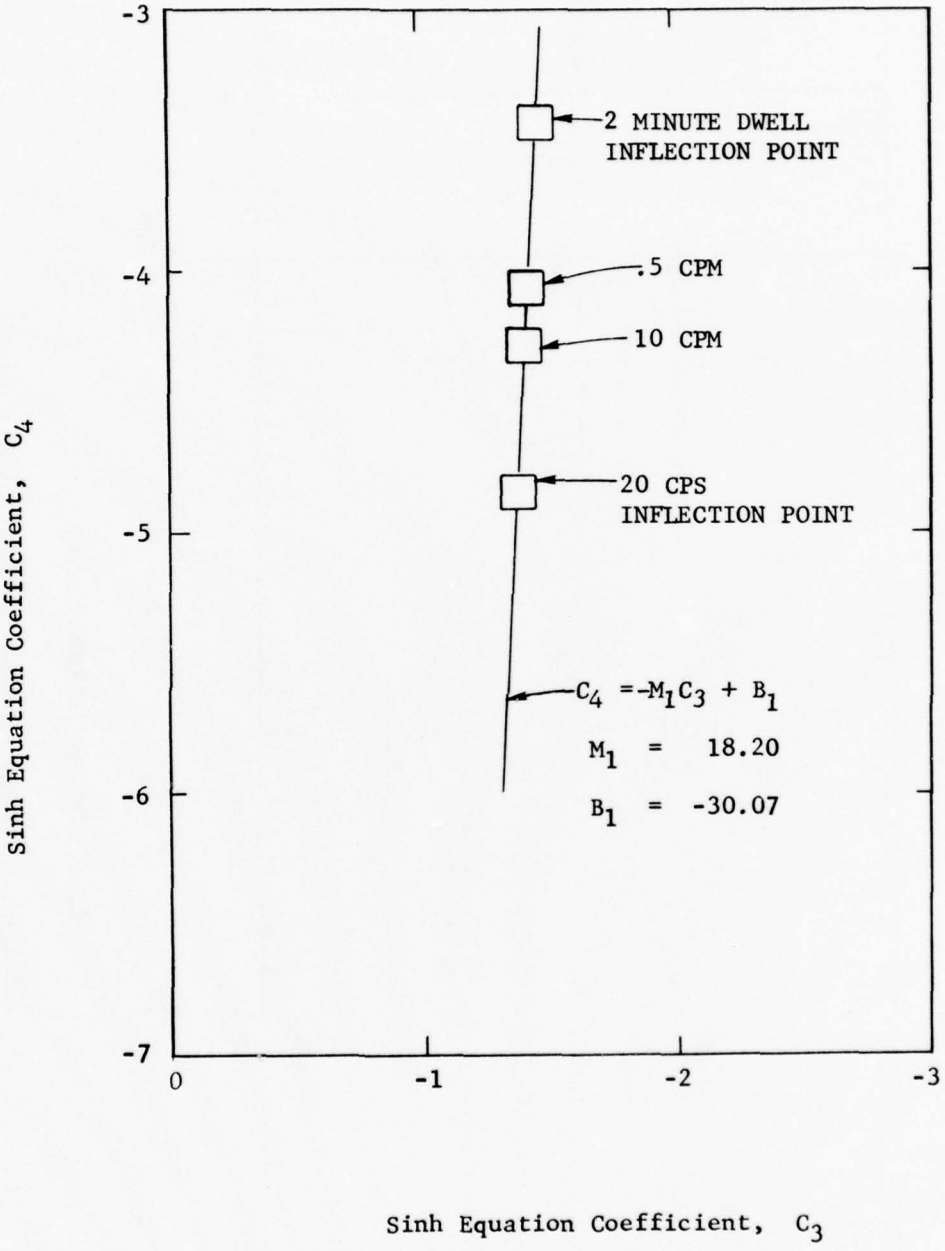

Figure 8. Relationship Between C_3 and C_4 for the Frequency Model

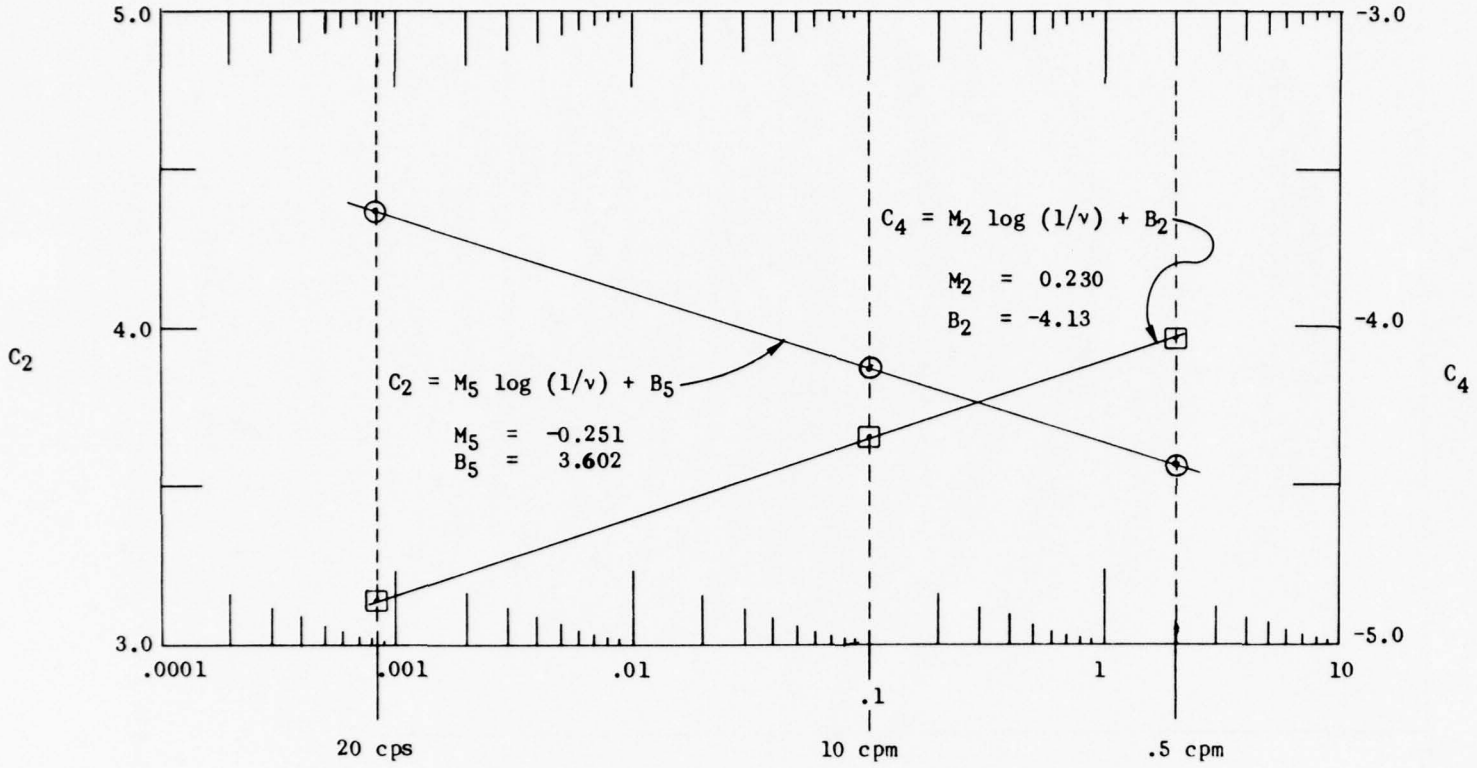

Figure 9. Effect of Frequency on Sinh Model Coefficients C_2 and C_4

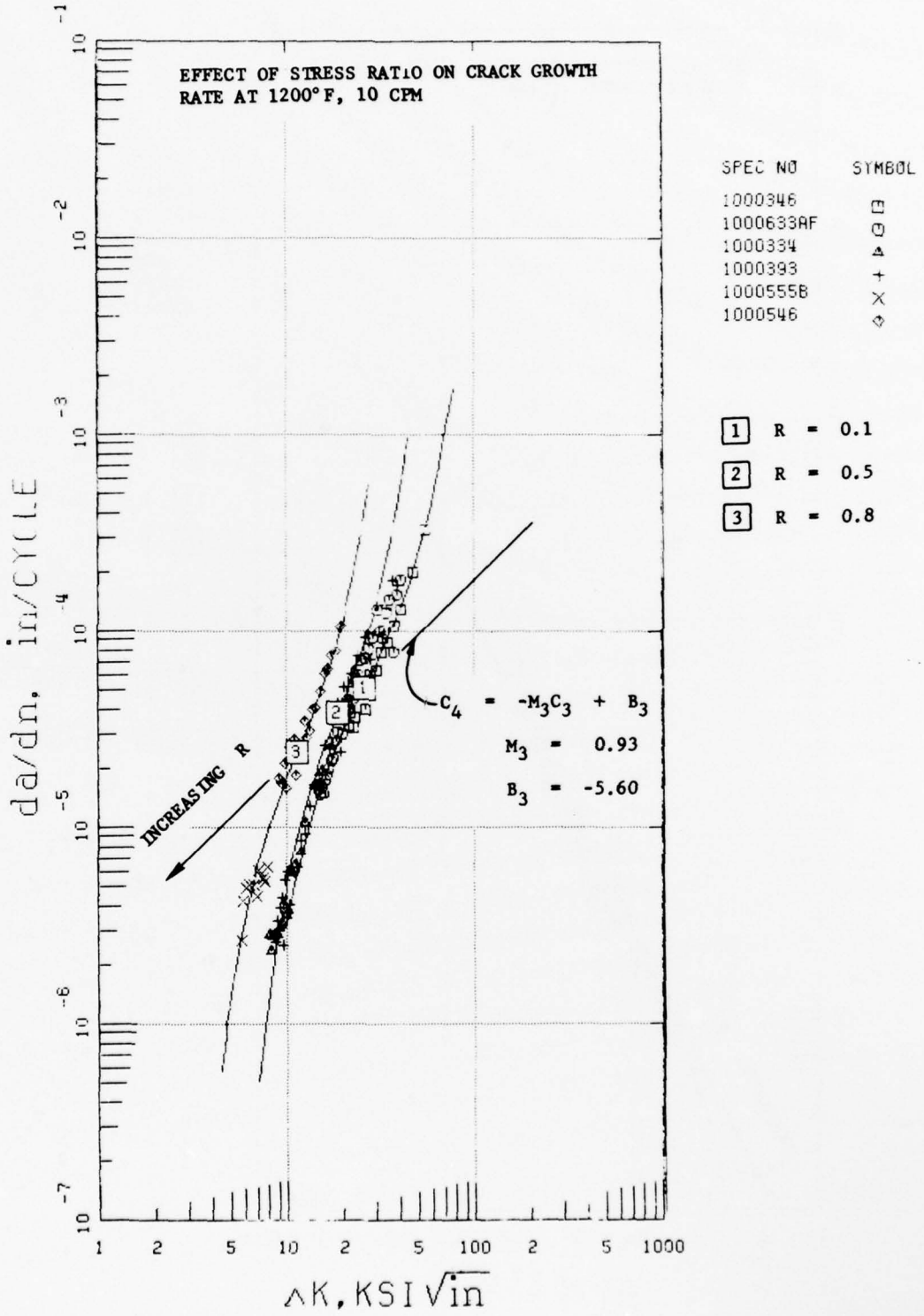

Figure 10. Effect of Stress Ratio on Crack Growth Rate at 1200°F, 10 cpm

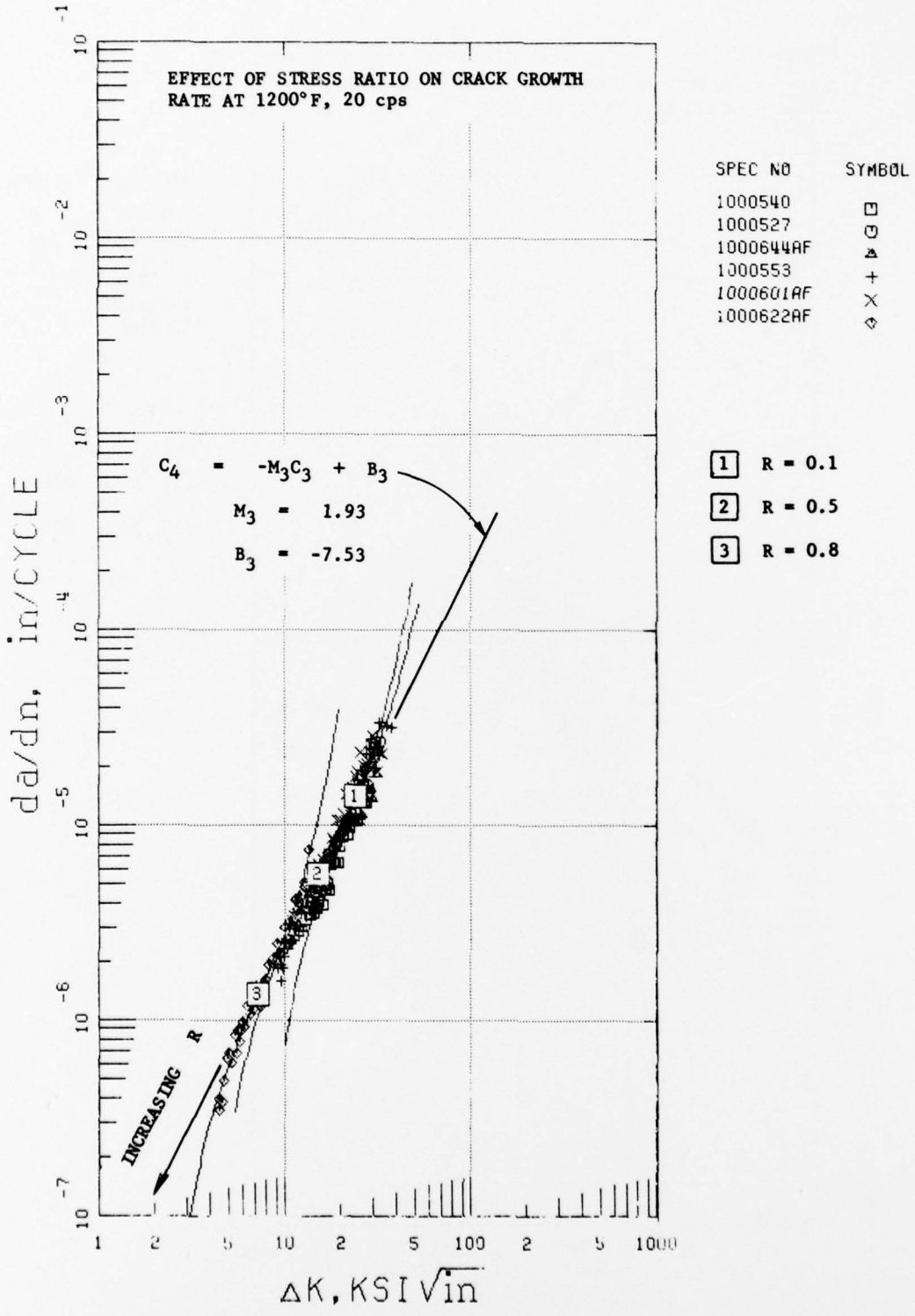

Figure 11. Effect of Stress Ratio on Crack Growth Rate at 1200°F, 20 cps

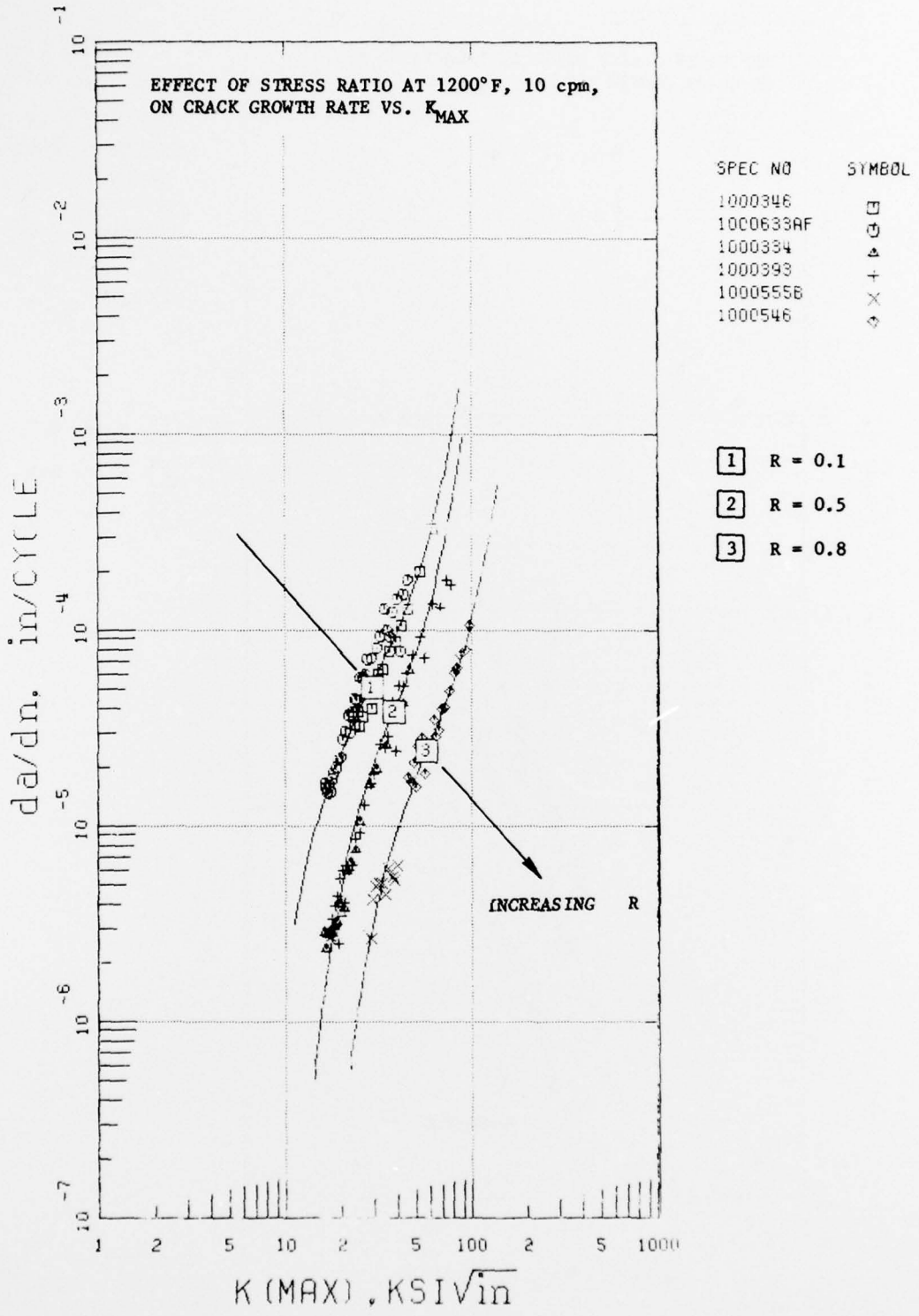

Figure 12. Effect of Stress Ratio at 1200°F, 10 cpm, on Crack Growth Rate vs K_{max}

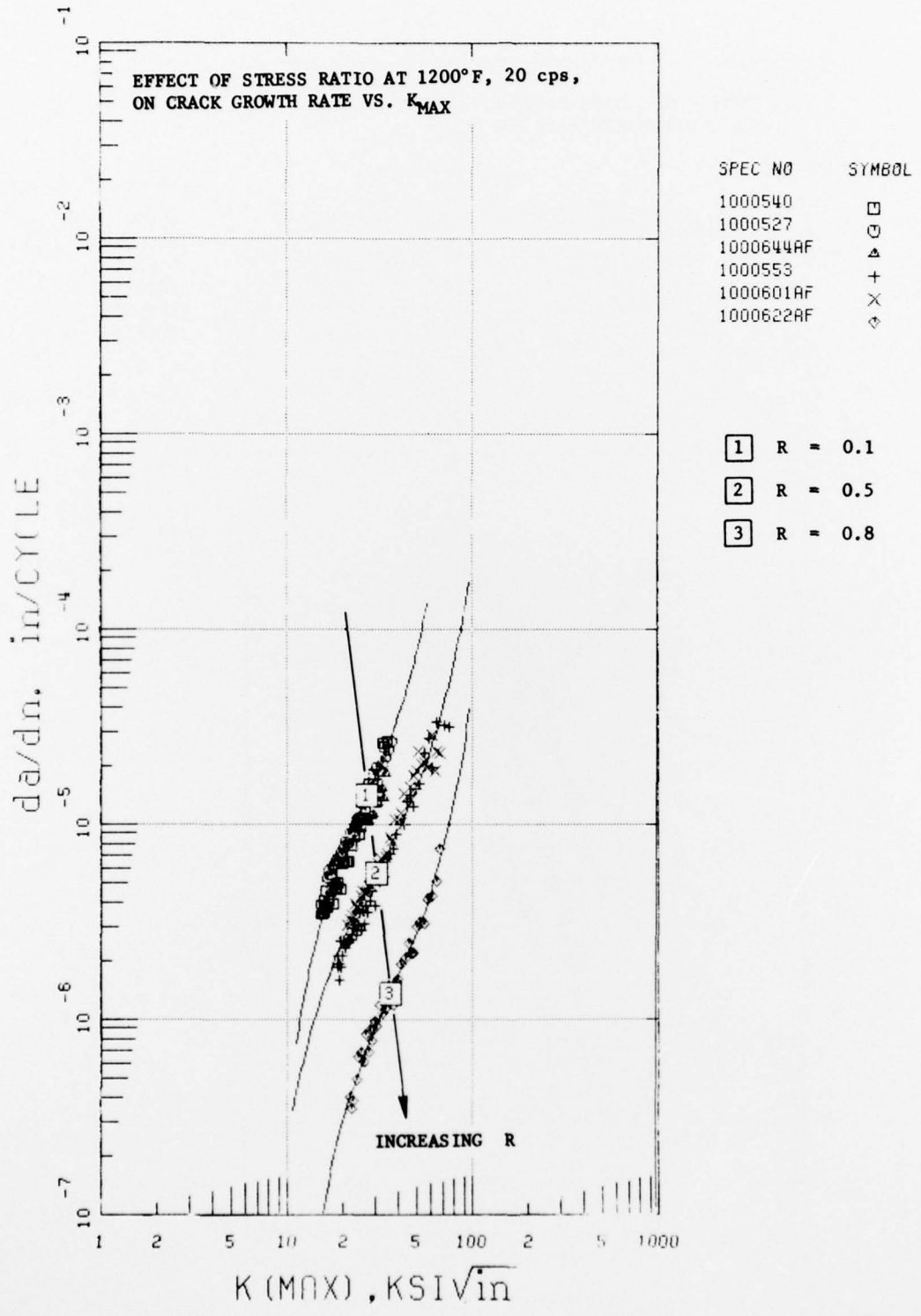

Figure 13. Effect of Stress Ratio at 1200°F, 20 cps, on Crack Growth Rate vs K_{max}

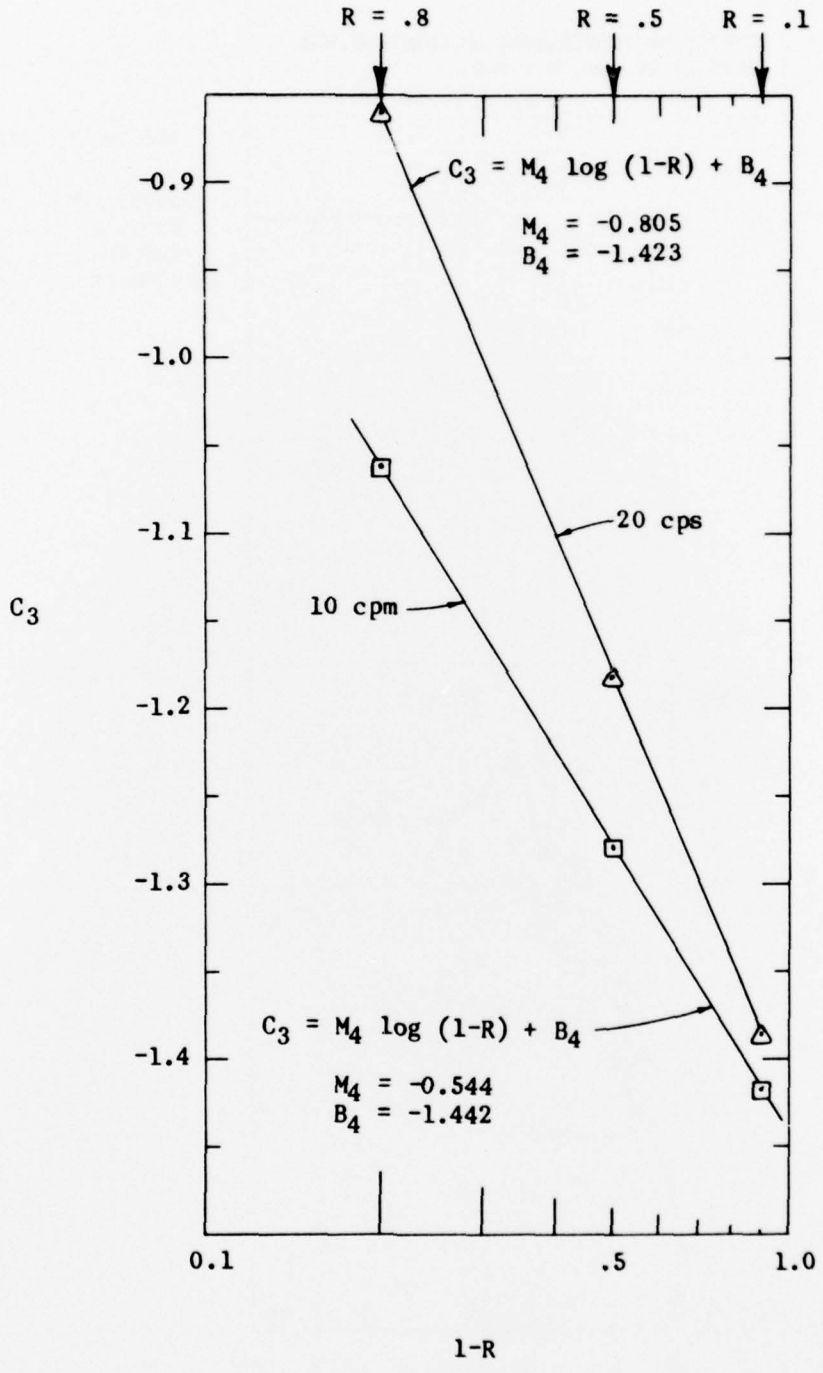

Figure 14. Effect of Stress Ratio, R, on Sinh Model Coefficient, C_3

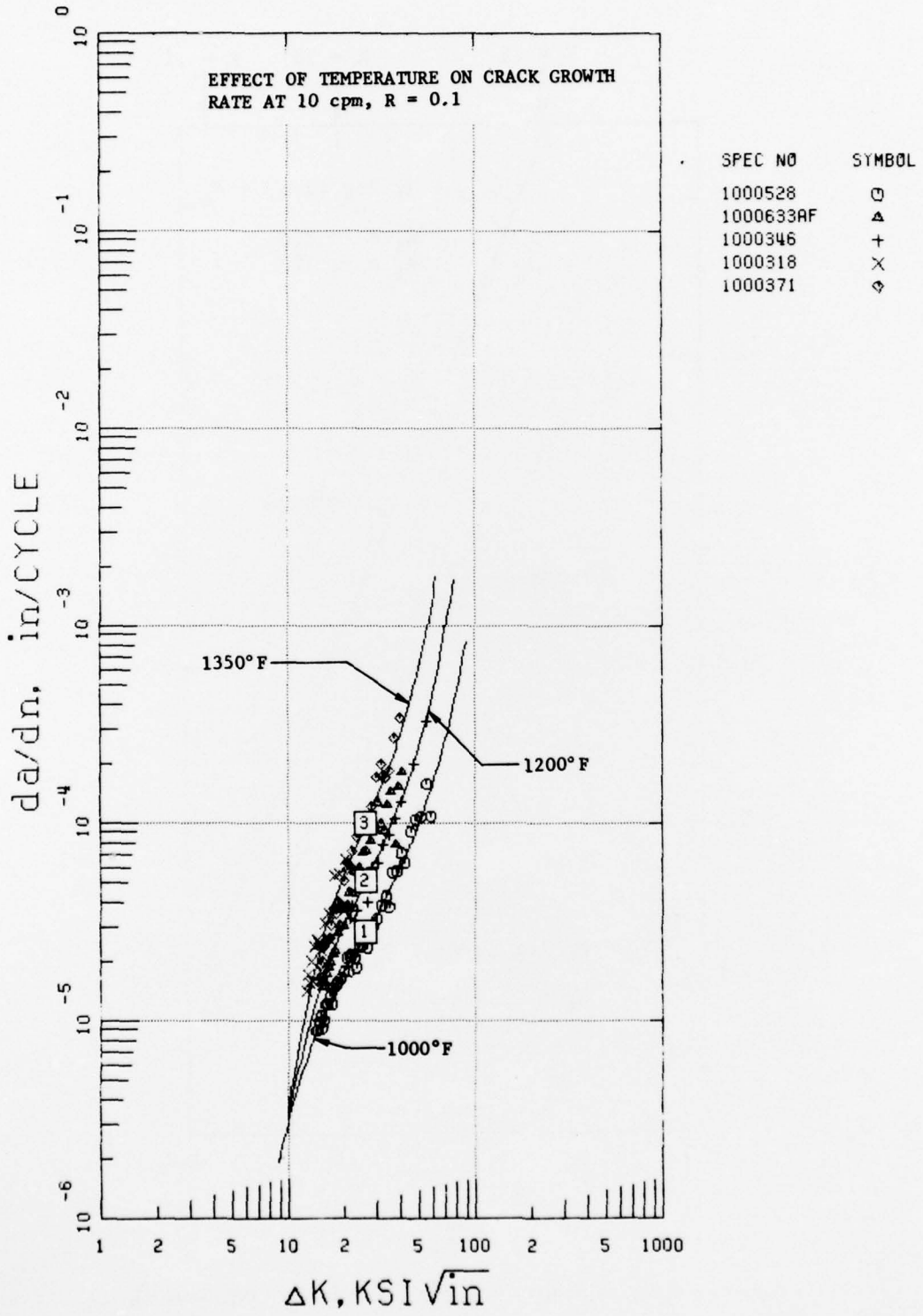

Figure 15. Effect of Temperature on Crack Growth Rate at 10 cpm, R = 0.1

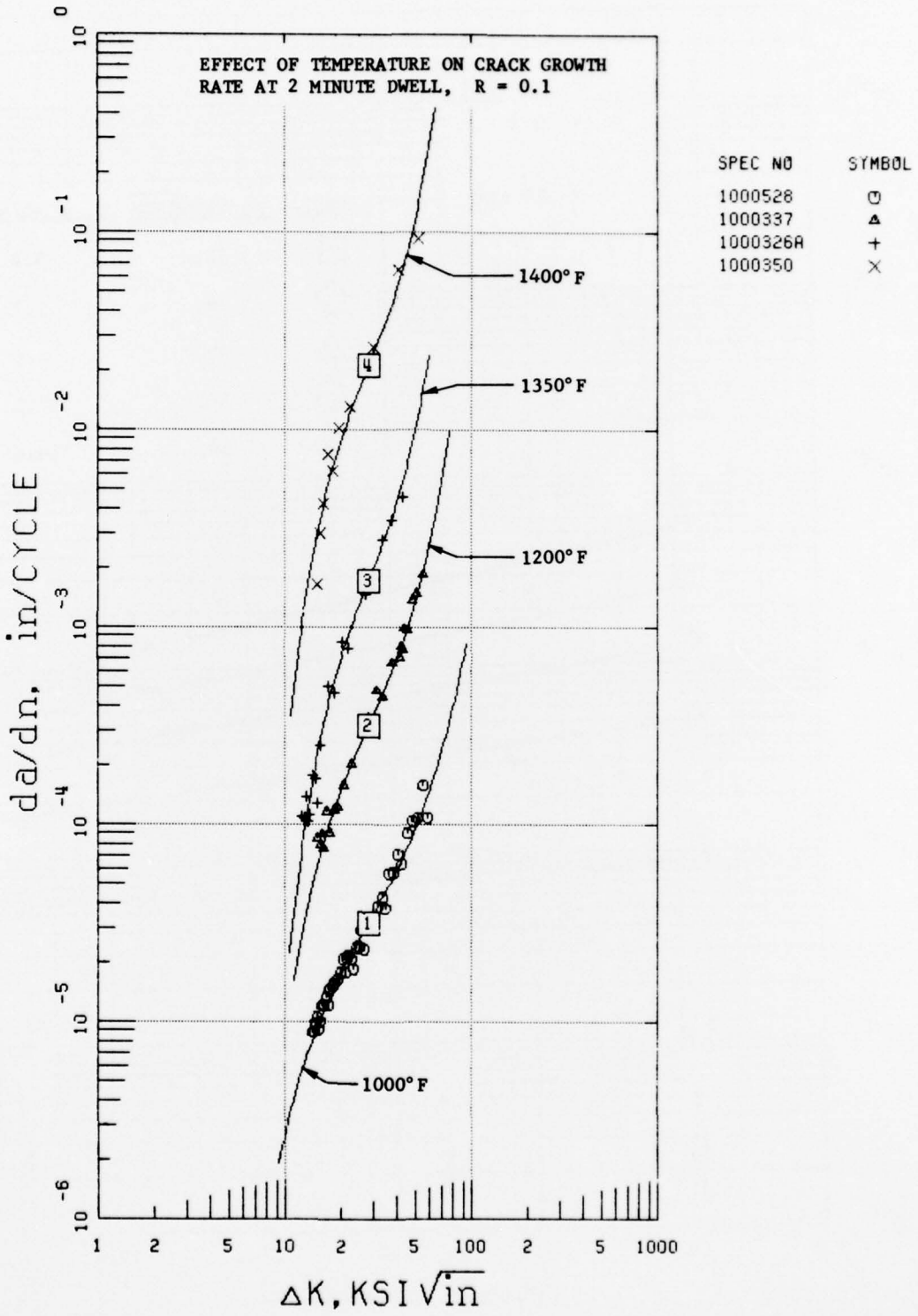

Figure 16. Effects of Temperature on Crack Growth Rate at 2 Minute Dwell, R = 0.1

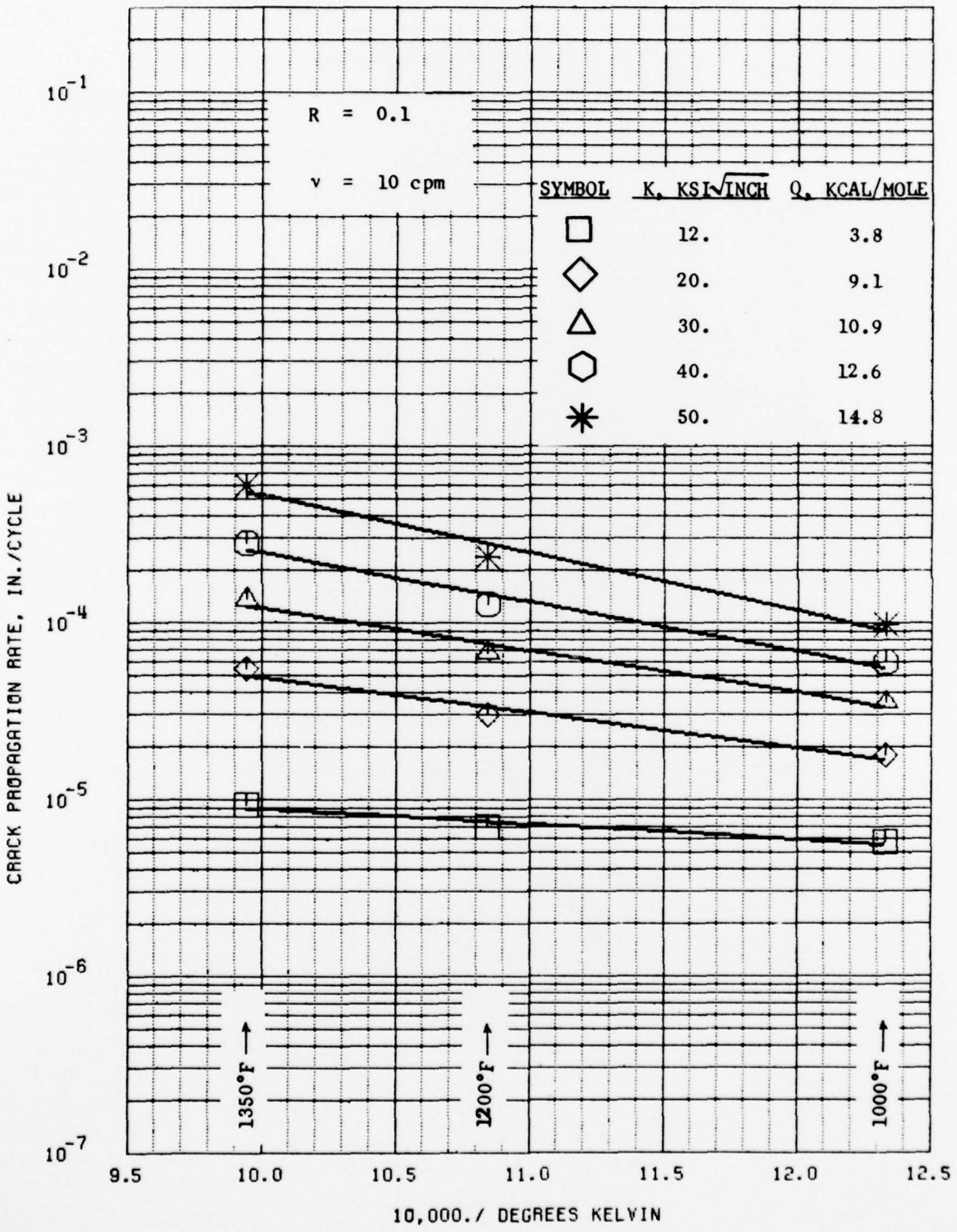

Figure 17. The Slope of Crack Propagation Rate vs Inverse Absolute Temperatue Is Proportional to Thermal Activation Energy, Q

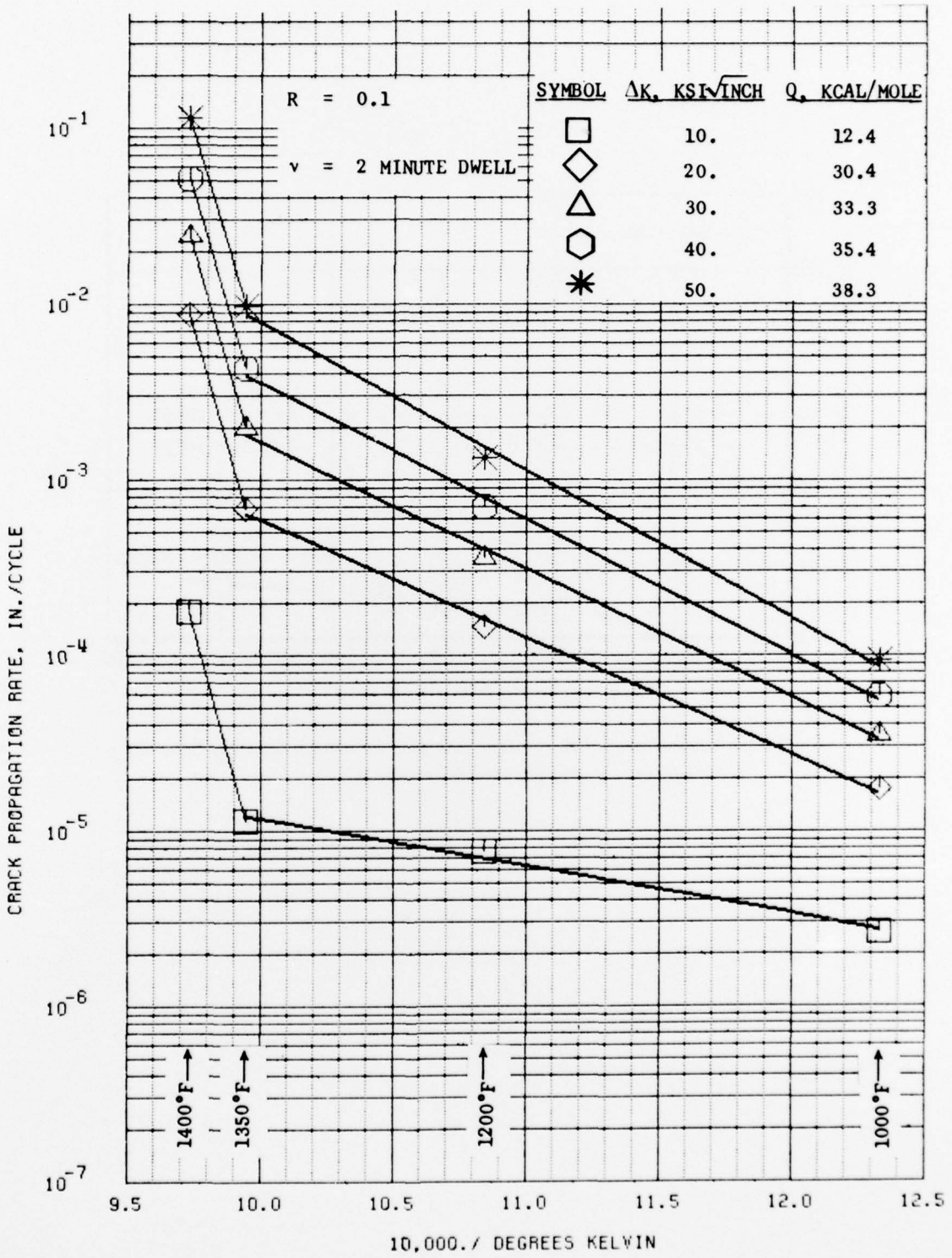

Figure 18. The Slope of Crack Propagation Rate vs Inverse Absolute Temperature Is Proportional to Thermal Activation Energy, Q

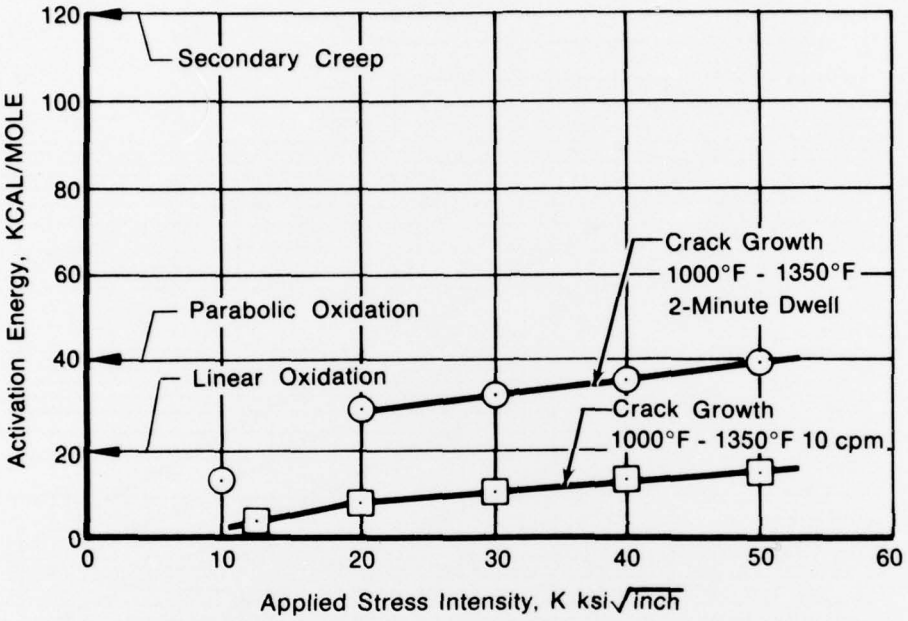

Figure 19. Comparison of Activation Energies for Crack Growth, Secondary Creep, Linear and Parabolic Oxidation

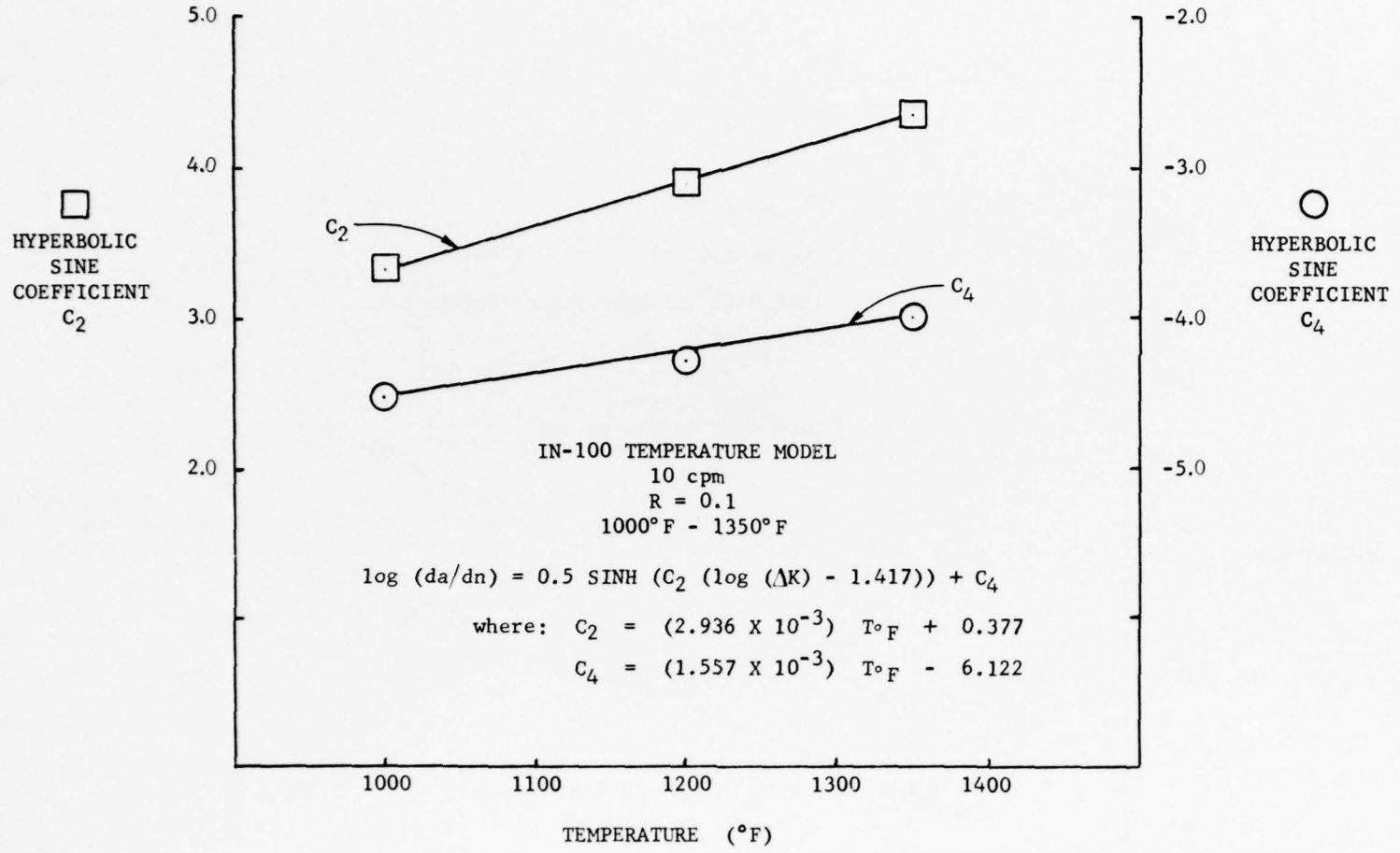

Figure 20. Effect of Temperature on Sinh Coefficients, 1000°F-1350°F, ν = cpm, R = 0.1

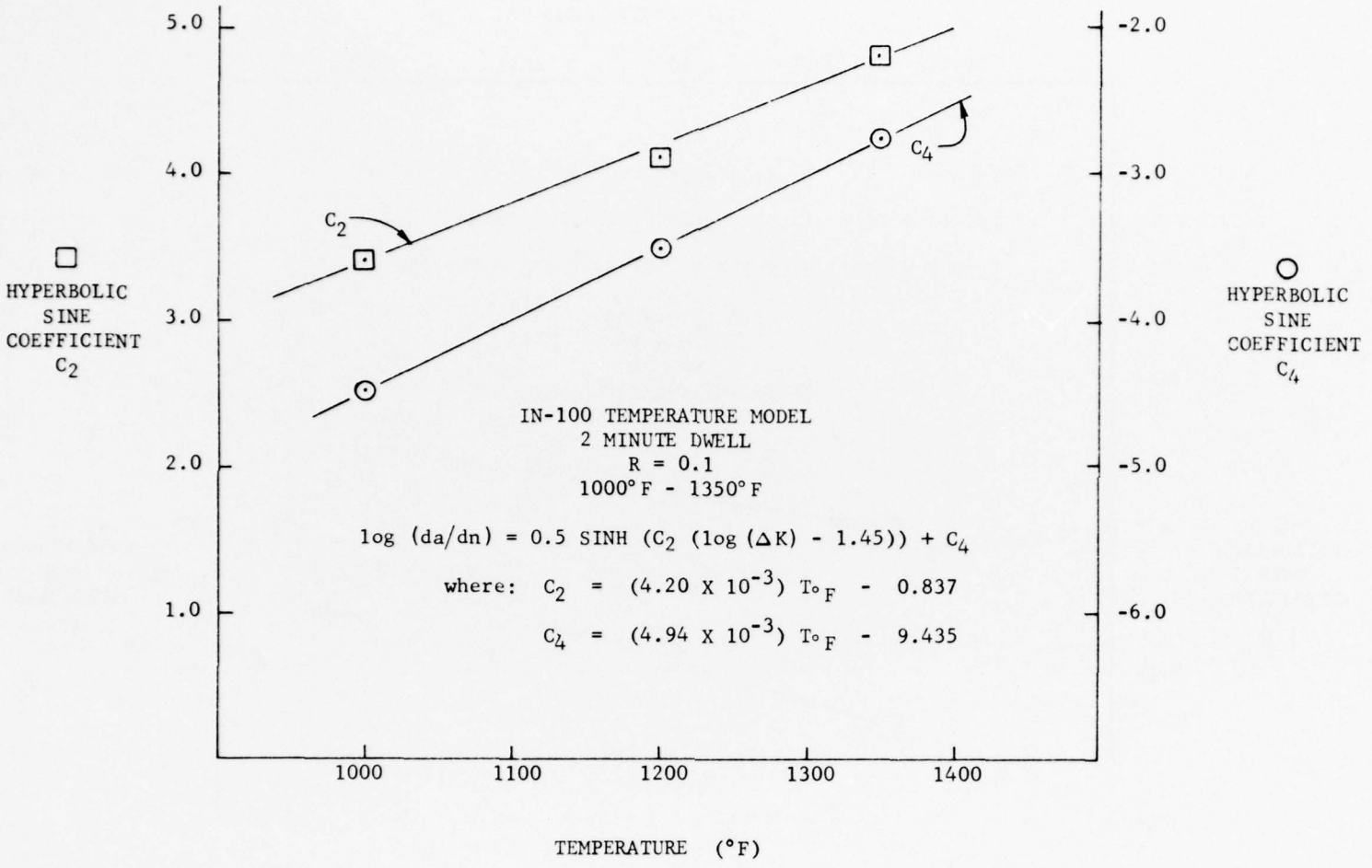

Figure 21. Effects of Temperature on Sinh Coefficients, 1000°F-1350°F, ν = 2 Minute Dwell, R = 0.1

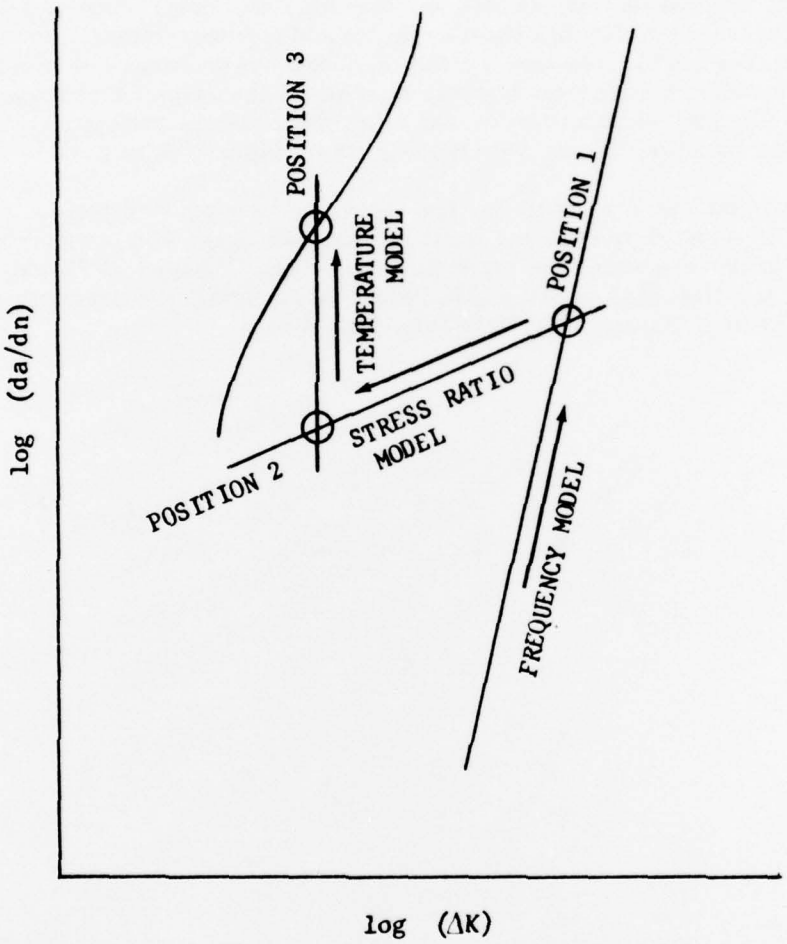

Figure 22. Schematic Representation of the Method for Determining Sinh Coefficients Representing Any Frequency, Stress Ratio, and Temperature

SECTION IV

CONCLUDING REMARKS

Experience acquired under Contract F33615-75-C-5097, Application of Advanced Fracture Mechanics at Elevated Temperatures, indicates some refinement of the model is necessary to account for the effects of heat-to-heat variations and specimen thickness. Investigations of the applicability of LEFM (Reference 3) to thin sections shows that some specimen tests used in the model development exhibit crack growth rates slower than expected of thicker specimens. In addition, it is now possible to distinguish subtle differences in crack propagation rates due to heat-to-heat variations. These model refinements are currently in progress.

The hyperbolic sine model has been shown to be a powerful tool for the interpolative analysis of elevated temperature crack propagation data. This methodology is used at P&WA/Florida to describe the crack propagation characteristics of IN-100, WASPALOY®, Astroloy, AF2-1DA, MAR-M-200, and IMI 4020. A stress ratio model is currently being developed for the advanced titanium alloy, Ti 6Al-2Sn-4Zr-6Mo.

REFERENCES

1. Shahinian, P., H. H. Smith, and H. E. Watson, "Fatigue Crack Growth Characteristics of Several Austenitic Stainless Steels at High Temperature," *Fatigue at Elevated Temperatures*, ASTM STP 520, American Society for Testing and Materials, 1973, pp. 387 - 400.

2. James, L. A., "The Effect of Frequency Upon the Fatigue-Crack Growth of Type 304 Stainless Steel at 1000°F," *Proceedings of 1971 National Symposium on Fracture Mechanics*, Part I, ASTM STP 513 pp. 218 - 229, 1972.

3. Wallace, R. M., C. G. Annis, and D. L. Sims, "Application of Fracture Mechanics at Elevated Temperatures," AFML Contract F33615-75-C-5097, Pratt & Whitney Aircraft Report FR-7506, March 1976.

4. Coffin, L. F., Jr., "Fatigue at High Temperature," *Fatigue at Elevated Temperatures*, ASTM STP 590, American Society for Testing and Materials, 1973, pp. 5-34.

☆ U. S. GOVERNMENT PRINTING OFFICE: 1977 — 757-001/280